

Fabricating 2D Silica with Atomic Layer Deposition

2018 CNF REU Intern: Reed Yalisove

2018 CNF REU Intern Affiliation:

Materials Science and Engineering, University of Michigan

CNF Project: 2018 Cornell NanoScale Science and Technology Facility Research Experience for Undergraduates Program

CNF REU Principal Investigator: Professor James R. Engstrom, Richard F. Smith School of Chemical and Biomolecular Engineering, Cornell University

CNF REU Mentor: Taewon Suh, Richard F. Smith School of Chemical and Biomolecular Engineering, Cornell University

Primary Source of CNF REU Funding: National Science Foundation via the National Nanotechnology Coordinated Infrastructure (NNCI) Grant No. ECCS-1542081

Contact: reedy@umich.edu, jre7@cornell.edu, ts695@cornell.edu

Website: http://www.cnf.cornell.edu/cnf_2018reu.html

Primary CNF Tools Used: Electron-beam evaporator, Oxford FlexAL ALD, general anneal 1 furnace, VCA contact angle, Woollam spectroscopic ellipsometer

Abstract:

Two-dimensional materials exhibit exciting new properties that could have applications for next-generation electronic devices. One such material is two-dimensional silica, called silicatene, which is an SiO_2 bilayer that only binds to a surface via van der Waals forces. Previous research has shown that silicatene can be made via evaporation of silicon and subsequent annealing in oxygen on a few single-crystalline metal surfaces, including Pd, Pt, and Ru. Atomic layer deposition (ALD) is a thin-film deposition technique used in the manufacturing of a variety of devices. This process repeats two self-limiting reaction steps to deposit a thin film, allowing angstrom-scale control of film thickness. The focus of this project was to investigate the use of ALD to deposit silicatene on several metal substrates. The metal substrates were deposited on silicon wafers via electron-beam assisted evaporation, and silica films were deposited with ALD. Post-deposition characterization of deposited film includes ellipsometry, contact angle, and x-ray photoelectron spectroscopy (XPS).

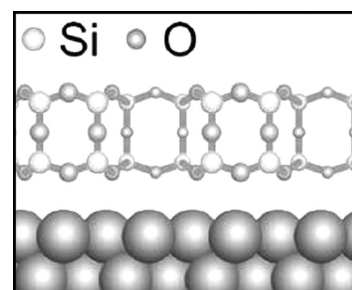


Figure 1: Figure adapted from ref. [1], the structure of silicatene. It consists of a bilayer of SiO_2 molecules attached to a metal substrate via van der Waals forces.

Introduction and Goals:

The thinnest stoichiometric arrangement of silica is a bilayer of silicon dioxide, known as silicatene. This material adheres to its substrate through van der Waals forces (see Figure 1). Silicatene has been fabricated on single crystal palladium (Pd), platinum (Pt), and ruthenium (Ru). Silicon (Si) was evaporated onto the metal substrate with an electron-beam assisted evaporator, then the films are annealed near 800°C and 10^{-6} mbar in an oxygen-rich environment [1]. Atomic layer deposition (ALD) is a thin-film deposition technique in which two self-limiting reactions are repeated, forming a film, atomic layer-by-atomic layer. This method allows low-temperature deposition of highly conformal, uniform films [2]. This research aimed to fabricate silicatene using atomic layer deposition.

Methods:

We chose Pd, Pt, and Ru as metal substrates for SiO_2 ALD. These metals were deposited on *p*-type silicon using an electron beam-assisted evaporator. Each metal film was 150\AA thick, and the Pt film was deposited on a 100\AA thick Ti adhesion layer on Si. Metal substrates [YR1] were characterized with contact angle and ellipsometry. SiO_2 films were deposited with ALD, using tris(dimethylaminosilane) (3DMAS) precursor and O_2 plasma as a co-reactant. Before the precursor was introduced, substrates were reduced in a H_2 plasma. Films were deposited at 200°C , with 5, 10, 20, 50, and 100 cycles of ALD. In addition, a “0 cycle” sample was created, which was not exposed to the Si precursor or the O_2 plasma, and a “20 second-half cycle” sample was created, which was not exposed to the 3DMAS, but did

undergo 20 cycles of the O_2 plasma co-reactant. Samples were annealed in an oxygen environment at 800°C for ten minutes at atmospheric pressure, then were allowed to cool to 300°C . Samples were characterized with contact angle, ellipsometry, x-ray photoelectron spectroscopy (XPS), and angle-resolved XPS (ARXPS) before and after annealing.

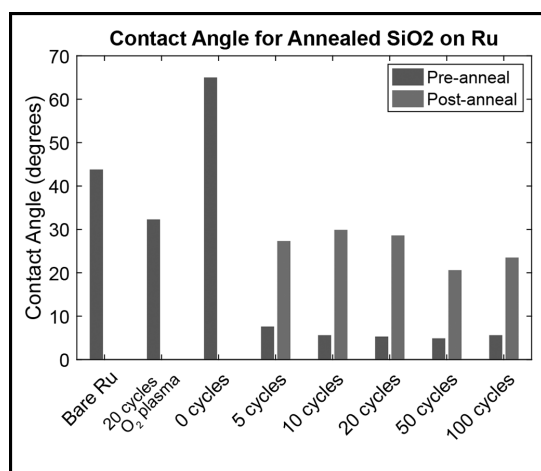


Figure 2: Contact angle data before and after annealing. Before annealing, contact angle is high without the introduction of Si precursor. When the Si precursor is introduced, the contact angle is consistently low. After annealing, the contact angle increases.

Results:

Contact angle showed high angles of water contact for the samples that were not exposed to the Si precursor (bare metal, 0 cycles, and 20 second-half cycles). The contact angles for the pre-annealed samples that were exposed to the Si precursor were uniform and low. This data shows that the exposure to the Si precursor caused a change on the sample surface, suggesting that SiO_2 was deposited. After annealing, contact angles were high, which is inconsistent with the expectation for silicatene. This trend (summarized in Figure 2) was observed for all three. Ellipsometry data shows a linear increase in thickness with the number of ALD cycles for all metal substrates, as seen in Figure 3. This suggests that we

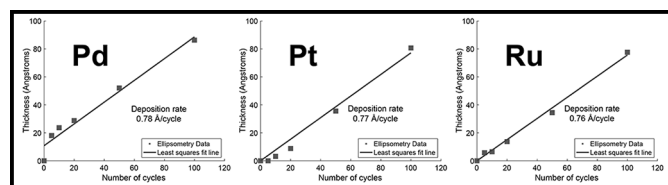


Figure 3: Ellipsometry data before annealing. All metals show a linear increase in thickness with number of ALD cycles.

observed normal ALD behavior, as the formation of silicatene would have led to an asymptote in the film thickness because it is unlikely the complete bilayer would have reacted with additional precursor due to the lack of dangling bonds. Ellipsometry data for the annealed samples was different than that of the pre-annealed samples, and it could not be fit to the expected models. XPS confirmed that the amount and thickness of SiO_2 increased with the number of ALD cycles. ARXPS showed that before annealing, our sample consisted of a thin film of SiO_2 on a buried Ru substrate. After annealing, ARXPS still showed a layer of SiO_2 on top of the sample but the morphology of Ru was inconclusive.

Conclusions:

XPS and ellipsometry suggest that silicatene was not produced. It is likely that during annealing, the SiO_2 combined with the metal to form metal silicides. This is supported by the change in contact angle after annealing and a study showing that Si will diffuse into metals, forming silicides [3]. This would also change the optical constants of the film, which caused the failure of the ellipsometry models.

Future Work:

Successful silicatene fabrication involved single crystal metal substrates [1], whereas our metal films were amorphous due to their evaporation. As a result, we would like to replicate this experiment on single-crystalline metal substrates.

Acknowledgements:

I would like to thank the CNF and its funding via the National Science Foundation NNCI Grant No. ECCS-1542081. Additionally, I would like to thank my PI, James R. Engstrom, and my mentor, Taewon Suh, for their willingness to give me a role in this research. I would like to give special thanks to Aaron Windsor for his patience and help with the evaporator, without which I would not have been able to complete my research.

References:

- [1] Büchner, C., and Heyde, M. (2017). Two-dimensional silica opens new perspectives. *Progress in Surface Science*, 92(4), 341-374.
- [2] George, S. M. (2010). Atomic Layer Deposition: An Overview. *Chemical Reviews*, 110(1), 111-131.
- [3] Petersson, C., Baglin, J., Dempsey, J., D'Heurle, F., and La Placa, S. (1985). Silicides of ruthenium and osmium: Thin film reactions, diffusion, nucleation, and stability. *Vacuum*, 35(6), 237.

Attonewton Sensitivity Magnet-Tipped Cantilevers and Sample Preparation for Single-Electron Spin Detection

CNF Project Number: 863-00

Principal Investigator: John A. Marohn

User: Peter (Hanyu) Sun

Affiliation: Department of Chemistry and Chemical Biology, Cornell University

Primary Source of Research Funding: Army Research Office

Contact: jam99@cornell.edu, hs859@cornell.edu

Website: marohn.chem.cornell.edu

*Primary CNF Tools Used: JEOL JBX-6300FS electron-beam lithography system,
CVC SC4500 e-gun evaporation system, Oxford PlasmaLab 80+*

Abstract:

Magnetic resonance force microscopy (MRFM) is a technique that increases sensitivity and resolution of magnetic resonance imaging beyond that achieved by traditional inductively-detected methods by using a nanomagnet-tipped cantilever as an attonewton-sensitivity force detector. In this report, we detail progress on magnet fabrication and sample preparation at the Cornell NanoScale Science and Technology Facility (CNF) that will enable single electron spin detection via MRFM.

Research Summary:

The Marohn group aims to use MRFM to image three-dimensional structures of biomolecular complexes that are hard to determine using techniques such as x-ray crystallography and cryo-electron microscopy. Achieving the signal-to-noise necessary to detect a single electron requires a nanomagnet with a large field-gradient to maximize the force and force-gradient between sample spins and the cantilever tip. The magnet-tipped cantilever fabrication protocol established by Longenecker separates the cantilever and magnet fabrication processes by depositing magnets first onto patterned chips instead of directly onto the cantilever (magnet-on-chip design) [1]. The fabricated magnet chip is then lifted-off from the wafer and attached to the cantilever with Omniprobe using a dual beam FEI Strata 400 STEM FIB system available at the Cornell Center for Materials Research (CCMR). The batch-serial process prevents the magnet from undergoing extreme conditions during the chemical etching process of the cantilever fabrication, reducing magnet damages. Magnet-tipped cantilevers produced this way have demonstrated record-high field gradients of 5 mT/nm [1], enabling many advances in detection and imaging.

In the past year work done at the CNF focused primarily on reproducing the fabrication protocol for cobalt-tipped cantilevers. The process involves 4-step e-beam lithography patterning on the JEOL JBX-6300FS electron-beam lithography system — alignment marks layout, chip structure, magnetic and under-etch patterning. The alignment and cobalt depositions were achieved with a CVC SC4500 e-gun evaporation system. The chip patterning and under-etch patterning were done in an Oxford PlasmaLab 80+ for silicon etching. The resulting magnet chips are shown in Figures 1 and 2.

The process allows for a 200 to 250 nm magnet overhang at the edge of the cantilever tip. The overhanging magnet design reduces surface noise caused by electrostatic interactions between fluctuating charges in the sample and the relatively large silicon surface of the cantilever tip. Reducing surface noise by increasing this silicon tip-sample separation is crucial to achieving the signal-to-noise necessary for detection and imaging. We are currently in the process of finishing a new batch of magnet-tipped cantilevers at the CCMR by attaching fabricated cobalt magnets onto previously prepared cantilevers.

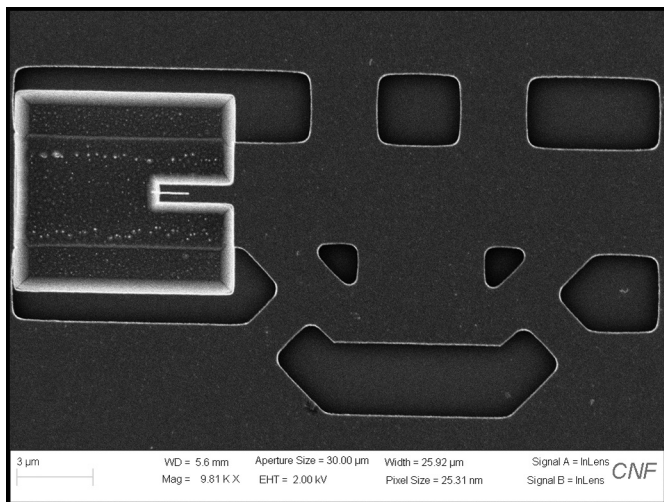


Figure 1: Magnet-on-chip design with an e-beam patterned cobalt. This specific pattern has a magnet of $\sim 1 \mu\text{m}$ in length, 80 nm in width and 200 nm in thickness. The overhang is $\sim 230 \text{ nm}$.

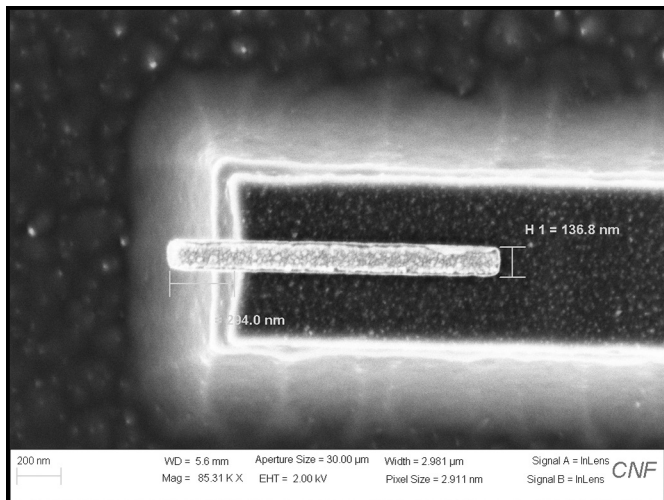


Figure 2: Cobalt magnet overhanging at the edge of the chip design. The magnet patterned is $\sim 1.2 \mu\text{m}$ long, 136 nm wide and 200 nm thick. The overhang is 294 nm .

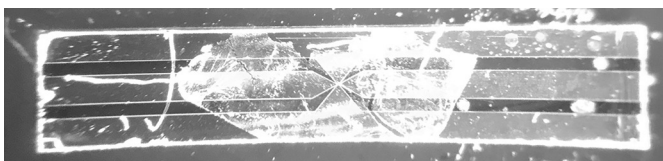


Figure 3: Multilayer graphene deposited on top of a coplanar waveguide spin-coated with a 200 nm thick polystyrene film. See full color version on pages xxviii-xxix.

To reduce surface noise for MRFM detection, the sample is coated with 12 nm gold film by e-gun deposition and wire-bonded to the ground plane to reduce surface charge accumulation. However, recent experiments suggest the e-gun deposition damages our nitroxide spin probes up to 20 nm in depth. One experimental approach is to use multilayer graphene as a replacement for gold due to its high electrical conductivity and mild conditions for transfer [2].

The substrate for growing multilayer graphene is a silicon wafer (290 nm oxide layer) with a 300 nm nickel film. The nickel film is deposited by the CVC SC4500 e-gun evaporation system at the CNF at a rate of 4 \AA/s . The graphene is then chemical vapor deposited at 900°C using the furnace from McEuen group (Department of Physics, Cornell University). The multilayer graphene is removed from the substrate and onto the surface of a water bath by a nickel etching process and directly scooped up onto a coplanar waveguide covered in a spin-coated sample. The resulting graphene-coated waveguide is shown in Figure 3. The properties of the graphene are characterized by an Asylum-MFP3D-Bio-AFM-SPM and a Renishaw InVia Confocal Raman microscope at the CCMR and the surface noise is then analyzed in our MRFM microscope.

We have yet to demonstrate surface noise comparable to e-gun deposited gold although more testing is needed. In addition, we are looking forward to further improving our magnet-tipped cantilever fabrication process in terms of increasing yield and reducing magnet damage to increase the sensitivity and resolution of our MRFM microscope.

References:

- [1] Longenecker, et al. ACS Nano 2012, 6 (11), 9637-9645.
- [2] Jo, G., et al. Nanotechnology, 2010, 21, 175201.

Investigation of Area Selective Atomic Layer Deposition with Microreactor and *in situ* Surface Analysis

CNF Project Number: 1239-04

Principal Investigator: James R. Engstrom

User: Taewon Suh

Affiliation: Robert Frederick Smith School of Chemical and Biomolecular Engineering, Cornell University

Primary Source of Research Funding: Semiconductor Research Corporation

Contact: jre7@cornell.edu, ts695@cornell.edu

Website: <http://engstromgroup.cbe.cornell.edu>

Primary CNF Tools Used: ALD, acid hoods

Abstract:

Atomic layer deposition (ALD) is a technique capable of precise control of film thickness and conformal film growth due to self-limiting nature of the precursors. Engstrom research group (ERG) has built a microreactor through which reactants of ALD are delivered and confined in a small region for deposition. This microreactor is coupled to an ultra high vacuum (UHV) chamber for surface characterization such that the deposited film is transferred *in vacuo*, without an air break, to the analysis chamber. In addition to the two reactants used in conventional ALD: ALD precursor and co-reactant, a third species called "co-adsorbate" is introduced for possible area selective deposition to act as a site-blocking layer.

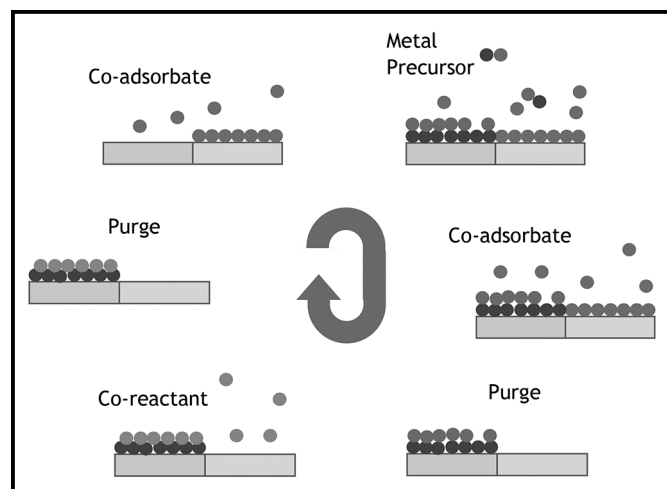


Figure 1: Schematic representation of an ALD cycle with co-adsorbate molecules.

Summary of Research:

In continuous downscaling of semiconductor devices, ALD has emerged as a potential approach capable of meeting required criteria of next generation technologies. The self-limiting nature of ALD precursors brings about two major advantages unique to the technique: precise control of thickness of deposited film and conformal growth [1]. ALD is sequential binary reaction separated by

purge steps to prevent any unwanted parasitic reactions between the precursor and co-reactant in gas phase. ERG takes this deposition technique a step further to study fundamental mechanisms involved in potential area selective ALD. Co-adsorbate molecules are introduced within a conventional cycle of ALD: before, during, and after precursor pulse as in Figure 1, to investigate how this third species potentially allows for area selective deposition. The deposited film is transferred *in vacuo* to and characterized in a UHV chamber coupled with the microreactor using x-ray photoelectron spectroscopy (XPS).

The thickness of deposited film (~ a few nm) is often in the range that is most effectively probed with surface-sensitive characterization techniques that require UHV, $p < 10^{-9}$ Torr. Conventional ALD is typically conducted at low to medium vacuum conditions ($p \sim 10^{-3}$ - 10^{-2} Torr), thus in most cases UHV-based analysis of the deposited thin films occurs in a separate chamber, requiring an air break that may significantly alter the surface composition, oxidation state, structure of the deposited film, and/or underlying substrate. Avoiding this air break is critical for fundamental studies of the growth of ultrathin films, particularly in the early stages. Figure 2 describes how a sample is exposed to precursors at the upper stage and transferred down to the lower stage of the chamber without exposure to air for post-deposition characterization.

In this report, we assess the feasibility of achieving area selective deposition with ALD by employing co-adsorbate molecules. Two substrates of different composition are used as initial surfaces: chemical oxide and metallic copper. Substrate preparation for the dielectric is conducted in the acid hood of CNF at Cornell University. This wet chemical etch includes submerging Si <100> wafer in buffered oxide etch (BOE) (6:1) for two minutes which produces hydrogen-terminated Si, confirmed by hydrophobicity of the surface. The substrate is then immersed in nanostrip for 15 minutes, which generates hydroxyl group termination with known density of $\sim 5 \times 10^{-14}$ OH/cm² [2]. This cycle of removing native oxide and generating chemical oxide is repeated twice. OH-terminated SiO₂ and copper substrates are loaded into the vacuum chamber within a sample holder as shown in Figure 3. This sample holder allows simultaneous exposure of substrates to reactants such that gas-surface reactions will occur under identical experimental conditions.

In area selective ALD experiments, substrates are annealed to substrate temperature of 180°C for an hour prior to exposure. Then co-adsorbate species is introduced to surfaces to form site-blocking layer to prevent incoming ALD precursor from adsorbing on undesired surfaces. The co-adsorbate molecules are present at relatively high ratio compared to ALD precursor during and after the precursor pulse to ensure area selective deposition. After purge of the precursor and co-adsorbate, pulse and purge of co-reactant occurs, just like in conventional ALD cycle. Deposited metal oxide films are characterized with *in situ* XPS using several parameters: photoionization cross section, inelastic mean free path, and kinetic energy, etc. [3]. The absolute atomic density of metal atom is calculated using calibration of semi-infinite Au film and methods described elsewhere [4].

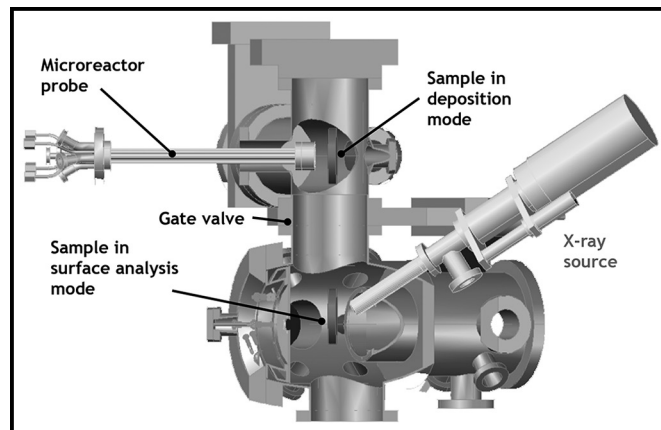


Figure 2: CAD rendering of the microreactor and UHV surface analysis chamber.

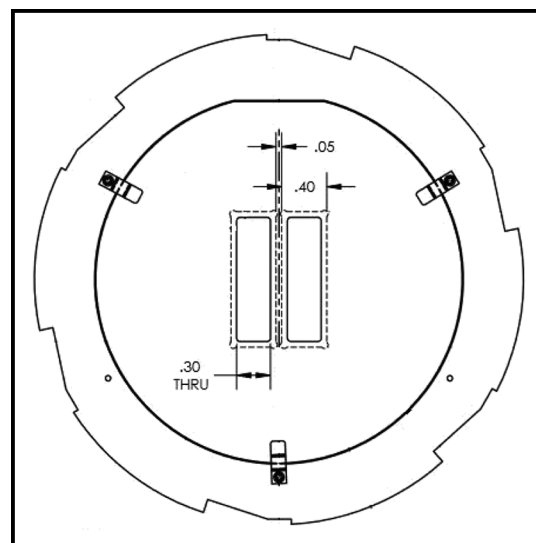


Figure 3: Sample holder capable of holding two copper samples.

References:

- [1] S. M. George, "Atomic layer deposition: An overview," *Chem. Rev.*, vol. 110, pp. 111-131, 2010.
- [2] L. T. Zhuravlev, "Concentration of hydroxyl groups on the surface of amorphous silicas," *Langmuir*, vol. 3, no. 3, pp. 316-318, 1987.
- [3] J. H. Scofield, "Hartree-Slater subshell photoionization cross-sections at 1254 and 1487 eV," *J. Electron Spectros. Relat. Phenomena*, vol. 8, no. 2, pp. 129-137, 1976.
- [4] K. J. Hughes and J. R. Engstrom, "Interfacial organic layers: Tailored surface chemistry for nucleation and growth," *J. Vac. Sci. Technol. A Vacuum, Surfaces, Film.*, vol. 28, no. 5, p. 1033, 2010.

Chemical Bonding Across the Periodic Table at High and Ambient Pressures

CNF Project Number: 1371-05

Principal Investigator: Roald Hoffmann

User: Guoying Gao

Affiliation: Department of Chemistry and Chemical Biology, Cornell University

Primary Source of Research Funding: National Science Foundation, Grant CHE-1305872

Contact: rh34@cornell.edu, gaoguoying@ysu.edu.cn

Website: <http://hoffmann.chem.cornell.edu/roald/>

Primary CNF Tools Used: CNF computer cluster

Abstract:

We address problems of bonding, structure, and emergent properties such as superconductivity in a wide range of materials — from discrete molecules through polymers to extended solids. The behavior of matter under high pressure is of special interest, as it forms a fruitful collaboration with the group of Neil Ashcroft in Physics. The specific project addressed in 2017-18 was the design of a new phase in the Si/C system, stoichiometry Si_3C .

Summary of Research:

As the second most abundant element in the Earth's crust, relatively low cost and an intrinsic semiconductor that can be both *n*- and *p*-doped, silicon has been widely used in the electronic industry. The well-known diamondoid Si(d-Si) structure is a semiconductor with an indirect gap of 1.2 eV and a much larger direct gap of 3.4 eV. As a consequence of the indirect gap nature of d-Si, Si solar cell absorber layers need to be relatively thick to absorb low energy photons. Much theoretical and experimental work has been directed toward the design and synthesis of direct band gap silicon allotropes, at 1 atm and under high pressure, preferably with a band gap value around optimal (~1.4 eV) for effective solar light conversion.

Si_3C is predicted to take on a diamondoid structure (space group: I-42d), at $P = 1$ atm, consistent with the experimental results on a cubic $\text{Si}_{0.75}\text{C}_{0.25}$ alloy. This structure is computed to be a semiconductor with a direct band gap of about 1.3 eV, a desired value. Under pressure, Si_3C may transform to metastable metallic R.3m-2 and R-3m-3 structures at about 25 and 250 GPa, respectively. Both are layered structures with six-coordinate Si and unusual six-coordinate carbon atoms.

The R-3m-1 and R-3m-2 structures (shown in Figure 1, along with the diamondoid structure) are both estimated to be superconductors with T_c of a few Ks. This is the first time that superconductivity in undoped silicon carbides is calculated.

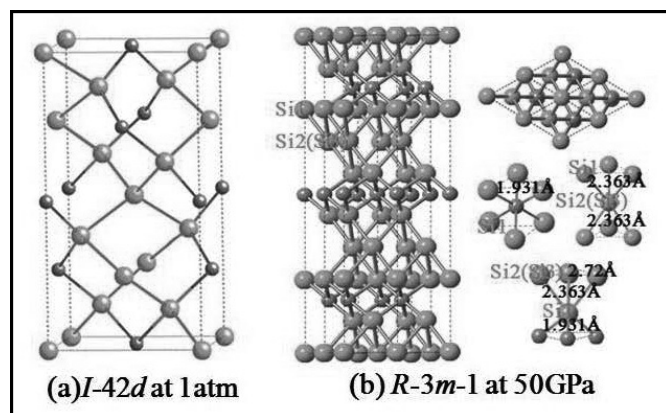


Figure 1: Predicted I-42d, and R-3m-1 structures for Si_3C at 1 atm, and 50 GPa, respectively. Orange, large balls are Si; grey, small balls carbon. The right panel of (b) presents the top view of the R-3m-1 structure and Si-or C-centered octahedra within the structure. See full color version on pages xxviii-xxix.

Substrate Preparation for Ultrafast Vibrational Spectroscopy Experiments

CNF Project Number: 1936-10

Principal Investigator: Poul B. Petersen

User: Stephanie Sanders

Affiliation: Department of Chemistry and Chemical Biology, Cornell University

Primary Source of Research Funding: National Science Foundation

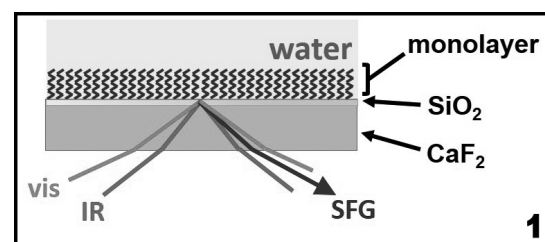
Contact: pbp33@cornell.edu, ses422@cornell.edu

Website: <http://petersen.chem.cornell.edu/>

Primary CNF Tools Used: Oxford ALD FlexAL

Abstract:

Water is ubiquitous and an active component in many natural and technological processes. Vibrational spectroscopy can be used to probe the structure and dynamics of water in a variety of environments. We use sum-frequency generation, a surface specific vibrational spectroscopy, to probe the structure and dynamics of interfacial water at chemically tunable surfaces. Interfaces with tunable surface character are created with self-assembled monolayers. In order to create substrates compatible for both silane self-assembly and sum-frequency generation, infrared and visible transparent CaF_2 windows are coated with SiO_2 . Then after surface functionalization with silane monolayers, the water structure and dynamics at the interfaces can be explored with sum-frequency generation.



Once the SiO_2 is deposited, hydrophobic, hydrophilic, or mixed monolayer are synthesized with self-assembly of silanes on the surface. Figure 1 shows a schematic of the surface in contact with water. Then, the surfaces and water at the surfaces are analyzed with SFG [2-5].

Summary of Research:

Water is an active component in many natural and technological processes [1]. Interfaces terminates the H-bonded network of water. We aim to study the structure and dynamics of water at self-assembled monolayers (SAMs) with varying surface character using sum-frequency generation (SFG) spectroscopy. In SFG, an infrared photon interacts with a dipole transition of the molecule and a visible photon excites the molecule to a virtual electronic state where it can undergo an anti-Stokes Raman transition resulting in a photon at the sum of the two incident frequencies being emitted [2,3]. In order to collect SFG spectra of solid-aqueous interfaces, we must probe through the window so the infrared photons are not absorbed by water. However, silica, a common SAMs substrate, also absorbs in the infrared.

To create an infrared and visible transparent substrate compatible with SAMs syntheses, we start with a CaF_2 window, which is transparent through the visible and infrared. Then approximately 10 nm of SiO_2 is deposited on the CaF_2 window via atomic layer deposition (ALD) with the Oxford ALD FlexAL. The SiO_2 layer is thin enough to not absorb all the IR photons and prevent SFG spectra of the sample from being collected, but thick enough to form a surface compatible with the self-assembly of silanes.

Once the SiO_2 is deposited, hydrophobic, hydrophilic, or mixed monolayer are synthesized with self-assembly of silanes on the surface. Figure 1 shows a schematic of the surface in contact with water. Then, the surfaces and water at the surfaces are analyzed with SFG [2-5].

References:

- [1] Ball, P. *Life's Matrix: A Biography of Water*; University of California Press: Berkeley, 2001.
- [2] Barrett, A. R.; Petersen, P. B. Order of Dry and Wet Mixed-Length Self-Assembled Monolayers. *J. Phys. Chem. C* 2015, 119 (42), 23943-23950.
- [3] Vanselous, H.; Petersen, P. B. Extending the Capabilities of Heterodyne-Detected Sum-Frequency Generation Spectroscopy: Probing Any Interface in Any Polarization Combination. *J. Phys. Chem. C* 2016, 120 (15), 8175-8184.175-8184.
- [4] Sanders, S.E.; Vanselous, H.; Petersen, P. B. Water at Surfaces with Tunable Surface Chemistries. *J. Phys. Condens. Matter* 2018, 30(11), 113001.
- [5] Kocsis, I.; Sorci, M.; Vanselous, H.; Murail, S.; Sanders, S.; Licsandru, E.; Legrand, Y-M.; van der Lee, A.; Baaden, M.; Petersen, P. B.; Belfort, G.; Barboiu, M. Oriented chiral water wires in artificial transmembrane channels. *Sci. Adv.* 2018 4(3), eaao5603.

A Thin Film Transfer Sample Preparation Technique for Single-Electron Magnetic Resonance Imaging

CNF Project Number: 2125-12

Principal Investigator: John A. Marohn

User: Michael Boucher

Affiliation: Department of Chemistry and Chemical Biology, Cornell University

Primary Source of Research Funding: Army Research Office

Contact: jam99@cornell.edu, mcb344@cornell.edu

Website: marohn.chem.cornell.edu

Primary CNF Tools Used: SC 4500 combination thermal/e-gun evaporation system

Abstract:

Magnetic resonance force microscopy (MRFM) is a type of scanning probe microscopy that uses the excellent force sensitivity of a silicon micro-cantilever in combination with spatially-resolved magnetic resonance made possible by the large local field gradient of the nanomagnet tip to image magnetic spins with theoretical sub-nanometer resolution. The primary goal of this research project is to advance the use of MRFM as a tool for imaging biomolecules and biomolecular complexes such as membrane proteins, whose structure is difficult to obtain by other means. Here we discuss recent developments in measurement sensitivity made possible through cantilever and waveguide fabrication performed at the Cornell NanoScale Science and Technology Facility (CNF) as well as new sample preparation techniques that will enable advances including electron paramagnetic resonance (EPR) detection of individual electron radical spin labels.

Summary of Research:

By employing nanomagnet-tipped attonewton-sensitivity cantilevers developed at the CNF in a magnetic resonance force microscopy (MRFM) measurement, the Marohn group has demonstrated the detection of 500 proton magnetic moments in a 1 mHz bandwidth [1]. In concert with a modified version of the spin modulation protocol first developed by Moore, et al. [2], these cantilevers should have the sensitivity required to image individual nitroxide spin labels on a single biomolecule or biomolecular complex with nanometer resolution.

A major challenge in performing such an experiment is mitigating cantilever frequency noise. One method that has proven effective in reducing this noise is applying a 10-20 nm thick metallic coating to the sample via electron-beam deposition to shield the cantilever from dielectric fluctuations in the sample. Proof-of-concept MRFM-EPR experiments performed on metal coated, tempamine-doped polystyrene samples, have demonstrated noise which is sufficiently low for imaging, however, have demonstrated significantly smaller signal than expected. Numerical simulations suggest the decreased spin signal is due to a 0.20 nm thick "dead layer" at the sample surface in which EPR active radicals are absent (Figure 1). Due to force-sensitivity limitations, this dead layer poses a significant challenge to MRFM detection of single electron spins.

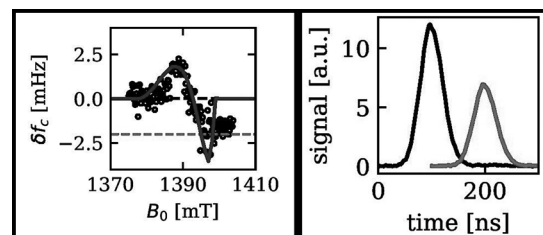


Figure 1, left: Electron spin resonance signal vs. applied magnetic field. The detection protocol developed by Moore, et al. detects the magnetic field gradient produced by sample spins as a modulated shift in the cantilever resonance frequency. Experimental results (black circles) from 30 seconds of signal acquisition, simulated signal of ~50 spins with a 20 nm dead layer (blue line) and expected frequency shift from a single electron near the sample surface (red dashed line).

Figure 2, right: Representative conventional pulsed-EPR measurement demonstrating a reduction in magnetic resonance signal from nitroxide spin probes which had been exposed to gold vapor deposition. Peaks are offset for clarity.

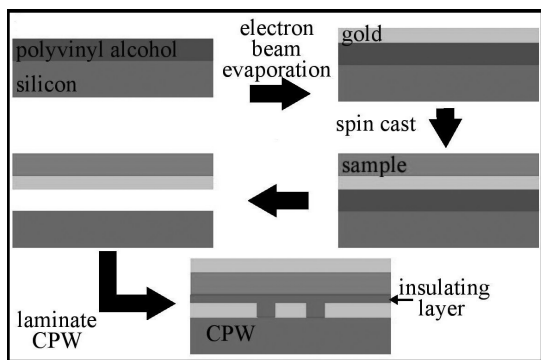


Figure 3: An outline of the sample/top contact transfer process that allows samples to be produced without exposing sensitive nitroxide electron radicals to physical deposition of the gold top contact.

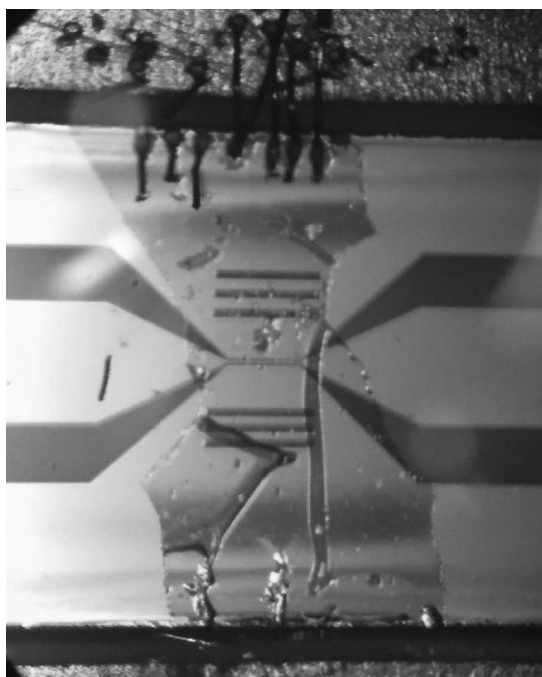


Figure 4: Optical image of a prepared sample/top contact over the tapered microwire region of the waveguide.

Using instrumentation at the National Biomedical Center for Advanced Electron Spin Resonance Technology to perform conventional EPR measurements on prepared 40 nm thick films using identical techniques, we have shown that the total EPR signal is reduced by about 50% after electron-beam vapor deposition of a 10 nm gold top layer — supporting our simulated estimations and suggesting that the process of gold deposition damages the spin probes in the uppermost layers of the sample (Figure 2).

To protect sample spins from direct exposure to the physical vapor deposition of the gold top contact, we developed a new sample preparation protocol. Figure 3 is a schematic of this protocol. A thin layer of polyvinyl alcohol is spin-coated onto a silicon substrate. A 10 nm thick layer of gold is then e-beam deposited on top of the PVA using the SC 4500 combination thermal/e-gun evaporation system at the CNF. The sample in this case, polystyrene doped with 40 mM tempamine, is then spin-coated on top of the gold layer. The Si/Au/polystyrene stack is then placed in a dish containing nanopure water that dissolves the PVA, allowing the Au/polystyrene layers to be transferred directly onto the waveguide to be used to deliver microwaves in the magnetic resonance experiment. Before the transfer, a thin layer of poly(methyl methacrylate) is spin-coated onto the waveguide to prevent shorting through the gold layer. We have found it necessary to transfer only a narrow strip of gold-coated sample because gold contact over the un-tapered region of the waveguide significantly reduces power transmitted through the waveguide. Recent room temperature measurements of the noise over these transferred sample top contacts have demonstrated frequency noise comparable to directly deposited samples.

Application of these newly prepared samples to detection/imaging experiments is currently underway.

References:

- [1] Longenecker, et al. ACS Nano 2012, 6 (11), 9637-9645.
- [2] Moore, et al. PNAS 2009, 106 (52), 22251-22256.

Study on the Electrochemically Stabilizing Effect of the High Dielectric Constant Oxide Artificial Solid Electrolyte Interphase on Electrodes in Aqueous Electrolytes

CNF Project Number: 2447-16

Principal Investigator: Lynden A. Archer

User: Yue Deng

Affiliation: Materials Science and Engineering Department, Cornell University

Primary Source of Research Funding: Private funding from Professor Archer

Contact: laa25@cornell.edu, yd339@cornell.edu

Primary CNF Tools Used: Oxford ALD FlexAL

Abstract:

Aqueous electrolytes, which have huge advantages in fire-hazard safety issues, are now still suffering from their narrow electrochemical stability windows. With the goal to study how ultra-thin oxide coatings can help to extend the stability windows of aqueous electrolytes, and more specifically, how band gap and dielectric constant affect the effectiveness of the oxide coatings, several high dielectric constant (k) metal oxides with different thicknesses were coated onto polished stainless-steel squares. The coated stainless-steel squares were then used to test the stability of aqueous electrolyte in a symmetric cell setup with one molar of lithium sulfate using cyclic voltammetry. The results show that an ultra-thin high k oxide layer helps to increase the stability window of the 1M Li_2SO_4 aqueous electrolyte to about five volts. However, no significant correlation between the width of the stability window and the dielectric constant or band gap of the coating materials was observed.

Summary of Research:

Artificial ultra-thin metal oxide was coated onto 1 cm by 1 cm polished stainless-steel squares (brought from McMaster-Carr Supply Company) by atomic layer deposition (ALD) [1] using the Oxford ALD FlexAL at Cornell NanoScale Science and Technology Facility (CNF). It has been shown in previous research that an ultra-thin (usually around 15 nm) alumina coating

on electrodes can largely increase the electrochemical stability of a rechargeable battery [2]. Therefore, two other high dielectric constant (k) metal oxides, silicon dioxide (SiO_2) and hafnium dioxide (HfO_2) [3], were applied at various thicknesses for studying. For each oxide coating, 1 nm, 5 nm, 10 nm, 15 nm, 20 nm, 25 nm, 30 nm, 35 nm, 45 nm, and 50 nm coatings were investigated. The cyclic

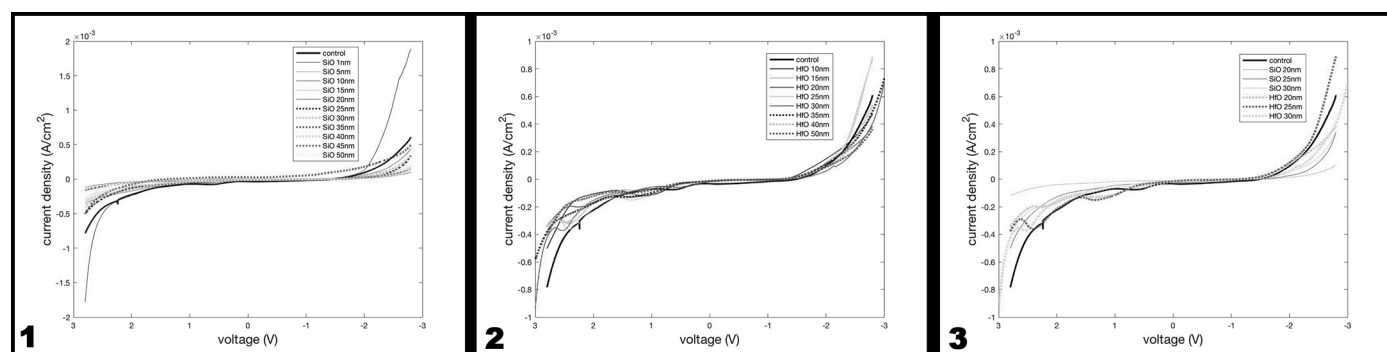


Figure 1, left: The cyclic voltammetry results for a typical symmetric SiO_2 coated stainless steel electrode versus SiO_2 coated stainless steel electrode cell with 1M aqueous lithium sulfate (Li_2SO_4) at various coating thicknesses. **Figure 2, middle:** The cyclic voltammetry results for a typical symmetric HfO_2 coated stainless steel electrode versus HfO_2 coated stainless steel electrode cell with 1M aqueous lithium sulfate (Li_2SO_4) at various coating thicknesses. **Figure 3, right:** A comparison between the cyclic voltammetry results for a symmetric SiO_2 coated half-cell and a symmetric HfO_2 coated half-cell with 1M aqueous lithium sulfate (Li_2SO_4) at various coating thicknesses.

voltammetry results for a typical symmetric SiO₂ coated stainless steel electrode versus SiO₂ coated stainless steel electrode cell with 1M aqueous lithium sulfate (Li₂SO₄) were summarized in Figure 1.

Figure 1 shows that, as the thickness of the SiO₂ layer increases, the stability window of the coin cell is improved. At 20 nm thickness, where the best stability is achieved, the stability window is increased from 3V (baseline generated by the uncoated stainless-steel control cell) to about 5V, which is about 66.7% improvement. For thicknesses beyond 20 nm, no further significant improvement is observed.

Figure 2 contains the cyclic voltammetry for the same coin cell setup with HfO₂ coating instead of SiO₂. Figure 2 proves that a thin layer of HfO₂ can also improve the stability of such aqueous electrolyte system, especially in the positive potential region. Different from SiO₂ coating, HfO₂ coating gives the best stability window enhancement at thickness around 35 nm. For HfO₂ coating that is thicker than 35 nm, no further significant improvement is observed.

Considering the results from both SiO₂ and HfO₂ coatings, it can be concluded that a semi-conducting or insulating protective layer can expand the stability window for an aqueous battery system. Initially, as the thickness of the coating increases, the stability window also increases. Until a certain thickness (25 nm for SiO₂ and 35 nm HfO₂), the stabilizing effect reaches its maximum and for thickness beyond this value, no further improvement can be achieved.

Figure 3 is a comparison between SiO₂ and HfO₂ coating. It shows that at the same thickness (which is thinner than 35 nm), the SiO₂ coating gives a wider stability window

than the HfO₂ coating does. Additionally, it is observed that there is a reaction peak around 2.2V for HfO₂ coated symmetric half-cell systems, while such a peak cannot be found on the SiO₂ coated symmetric half-cell system. This might indicate that the HfO₂ coating reacts with water or aqueous Li₂SO₄ solution at 2.2V, which suggests that SiO₂ is a more stable coating material to be used in aqueous electrolyte system.

The SEM results of cycled coated electrodes provide evidence. After 11 cyclic sweeps, no HfO₂ could be found at the surface of the electrodes, but SiO₂ was still found evenly covering the entire surface. However, further investigation on the electrolytes after cyclic sweeps is required to make a solid conclusion.

Based on these results, neither band gap nor dielectric constant of the oxide coating has a dominating effect on its ability to stabilize the aqueous system. The chemical reactivity of the coating material against the electrolyte is the crucial factor. Studies of other high κ oxides, such as silicon nitride and hafnium silicate, can help to confirm this hypothesis.

References:

- [1] Jung, Y. S.; Cavanagh, A. S.; Dillon, A. C.; Groner, M. D.; George, S. M.; Lee, S.-H. Enhanced Stability of LiCoO₂ Cathodes in Lithium-Ion Batteries Using Surface Modification by Atomic Layer Deposition. *J. Electrochem. Soc.* 2010, 157 (1), A75.
- [2] He, Y.; Yu, X.; Wang, Y.; Li, H.; Huang, X. Alumina-Coated Patterned Amorphous Silicon as the Anode for a Lithium-Ion Battery with High Coulombic Efficiency. *Adv. Mater.* 2011, 23 (42), 4938-4941.
- [3] Robertson, J. Band Offsets of Wide-Band-Gap Oxides and Implications for Future Electronic Devices. *J. Vac. Sci. Technol. B Microelectron. Nanom. Struct.* 2000, 18 (3), 1785.

Measuring Refractive Index of Microscopy Slides

CNF Project Number: 2673-18

Principal Investigator: Peng Chen

User: Xiangcheng Sun

Affiliation: Department of Chemistry and Chemical Biology, Cornell University

Primary Source of Research Funding: Army Research Office

Contact: pc252@cornell.edu, xs266@cornell.edu

Primary CNF Tools Used: Accurion EP3 imaging ellipsometer, Metricon prism coupler

Abstract:

There are plenty of tools that Cornell NanoScale Facilities (CNF) possesses on materials characterization, which is of vital importance to research. In this project, when we measure the refractive index of the microscopy slides (suspected materials), the CNF refractometer, ellipsometer and Metricon prism coupler were considered to be useful. Finally, Metricon prism coupler was used to measure the refractive index of the material, and the refractive index was obtained under a series of wavelengths. We also used the Cauchy model in that it derived to propose the relation of the refractive index of material with the relation of light wavelengths. Through this study, we verified that the materials measured were the exact ones we would like to study.

Summary of Research:

In this research, materials characterization is of vital importance, and the tool set at Cornell NanoScale Facility (CNF) did just the job that what we needed as there are plenty of tools that help researchers with characterization.

Our project is working on the visualization of single polymer growth using single-molecule fluorescence imaging. Total internal reflection fluorescence microscopy is utilized. We're using sapphire and quartz microscopy slides and prisms, the properties of which are of great importance to our experiments. Especially, the refractive index of materials affects the light path in the materials greatly, which should be known clearly in this research.

Different tools (such as refractometer, ellipsometer and Metricon prism coupler) were considered to measure the refractive index of the slide materials. Firstly, Accurion EP3 imaging ellipsometer was applied to measure the refractive index of bulk materials (microscopy slides). After a series of experiments, it was found that it is challenging to get refractive index of slides through ellipsometry. Generally, ellipsometers are able to measure the thickness or refractive index of a thin layer on the known substrate [1]. This thin layer might include metal

films, oxides, organic coatings or biological molecule layer such as DNA [2]. For our target materials, slides are the bulk materials.

The Metricon model 2010/M prism coupler utilizes advanced optical waveguiding techniques to rapidly and accurately measure both the thickness and the refractive index/birefringence of dielectric and polymer films as well as refractive index of bulk materials. The 2010/M offers unique advantages over conventional refractometers and instruments based on ellipsometry [3,4]. For example, unlike most conventional refractometers, which are single-wavelength (typically 589 nm), the 2010/M can be equipped with as many as five lasers, allowing easy measurement of dispersion across a wide wavelength range.

The Metricon prism coupler was used to measure the refractive index of the material and the refractive index was obtained. We also used Cauchy model in that it derived to propose the relation of the refractive index of material with the relation of light wavelengths. The refractive index values from the Metricon were obtained and shown as follows:

n@446nm: 1.77734

n@637nm: 1.76311

n@824nm: 1.75705

n@1059nm: 1.75287

n@1058nm: 1.74434

With the refractive index at different wavelengths, the Cauchy model was used to fit the data [5], and the equation between refractive index (n) and light wavelength (.) was obtained and shown as follows.

$$n = 1.7412 + 1.2954 \times 10^4 \lambda^{-2} - 1.1617 \times 10^9 \lambda^{-4} \quad (1)$$

Figure 1 shows the measured refractive index under different wavelength and the fitting Cauchy equation. The obtained refractive index of our microscopy slide is consistent with the reported refractive index of sapphire materials.

Through this process, we verified that the materials measured were the exact ones we would like to study.

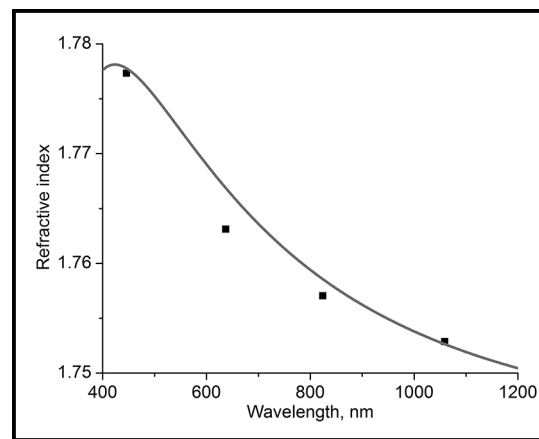


Figure 1: Measured refractive index of the microscopy slide under different wavelength and the corresponding fitting using Cauchy model.

Acknowledgements:

We greatly appreciate the funding from Army Research Office. Xiangcheng Sun thanks the help from CNF staff member, Jeremy Clark.

References:

- [1] Frank L. McCrackin, Elio Passaglia, Robert R. Stromberg, and Harold L. Steinberg, Measurement of the Thickness and Refractive Index of Very Thin Films and the Optical Properties of Surfaces by Ellipsometry, *Journal of Research of the National Bureau of Standards – A. Physics and Chemistry*, 1963, 67A, 363. Janos Vörös, The Density and Refractive Index of Adsorbing Protein Layers, *BioPhysical Journal*, 2004, 87, 553.
- [2] Steven T. Kirsch, Determining the refractive index and thickness of thin films from prism coupler measurements, *Applied Optics*, 1981, 20, 2085.
- [3] J Cardin, D Leduc, Determination of refractive index, thickness, and the optical losses of thin films from prism-film coupling measurements, *Applied optics*, 2008, 47, 894.
- [4] F.A. Jenkins and H.E. White, *Fundamentals of Optics*, 4th ed., McGraw-Hill, Inc. (1981).
- [5] Elena R. Dobrovinskaya, Leonid A. Lytvynov, Valerian Pishchik, *Sapphire Material, Manufacturing, Applications*, Springer (2009).